

Supplementary Material

Ioannis A. Nellas¹, Sotiris K. Tasoulis¹,
Vassilis P. Plagianakos¹ and Spiros V. Georgakopoulos²

¹*Department of Computer Science and Biomedical Informatics
University of Thessaly, Greece*

²*Department of Mathematics
University of Thessaly, Greece*

{inellas, stas, vpp, spirosgeorg} @uth.gr

September 7, 2022

Contents

1	Latent Space Analysis	1
1.1	Experimental Results	1
1.2	Latent Space Visualization	1

1 Latent Space Analysis

1.1 Experimental Results

Table 1: Performance Comparison of CSAE for different number of dimensions (denoted as λ) in the Latent Space.

	MNIST		Fashion MNIST		Brain Tumor Dataset		SARS-COV-2 CT-Scans	
	Accuracy	Weighted F1-Score	Accuracy	Weighted F1-Score	Accuracy	Weighted F1-Score	Accuracy	Weighted F1-Score
$\lambda = 2$	0.9751	0.9750	0.8959	0.8961	0.9575	0.9574	0.9436	0.9436
$\lambda = \#classes$	0.9871	0.9871	0.9117	0.9114	0.9510	0.9510	0.9436	0.9436
$\lambda = 16$	0.9892	0.9891	0.9113	0.9113	0.9331	0.9318	0.9336	0.9335
$\lambda = 32$	0.9889	0.9888	0.9088	0.9088	0.9494	0.9495	0.9175	0.9174
$\lambda = 64$	0.9892	0.9891	0.9127	0.9125	0.9526	0.9527	0.9356	0.9356
$\lambda = 128$	0.9903	0.9902	0.9141	0.9138	0.9331	0.9316	0.9315	0.9315

Table 2: Performance Comparison of the execution of traditional classification methodologies onto the Latent Representations constructed by CSAE for different number of dimensions (denoted as λ) in the Latent Space and the flattened images.

	MNIST		Fashion MNIST		Brain Tumor Dataset		SARS-COV-2 CT-Scans	
	Accuracy	Weighted F1-Score	Accuracy	Weighted F1-Score	Accuracy	Weighted F1-Score	Accuracy	Weighted F1-Score
CSEA L.S. + kNN								
$\lambda = 2$	0.9785	0.9784	0.9245	0.9241	0.9624	0.9625	0.9657	0.9657
$\lambda = \#classes$	0.9926	0.9925	0.9309	0.9303	0.9657	0.9656	0.9657	0.9657
$\lambda = 16$	0.9921	0.9920	0.9348	0.9641	0.9638	0.9625	0.9557	0.9557
$\lambda = 32$	0.9932	0.9931	0.9339	0.9334	0.9575	0.9571	0.9597	0.9597
$\lambda = 64$	0.9931	0.9930	0.9360	0.9357	0.9673	0.9672	0.9476	0.9476
$\lambda = 128$	0.9940	0.9939	0.9334	0.9330	0.9641	0.9638	0.9436	0.9436
CSEA L.S. + SVM								
$\lambda = 2$	0.9758	0.9758	0.8959	0.8964	0.9608	0.9607	0.9436	0.9436
$\lambda = \#classes$	0.9872	0.9871	0.9157	0.9152	0.9510	0.9510	0.9436	0.9436
$\lambda = 16$	0.9889	0.9888	0.9146	0.9143	0.9429	0.9428	0.9396	0.9396
$\lambda = 32$	0.9893	0.9892	0.9130	0.9129	0.9429	0.9428	0.9295	0.9295
$\lambda = 64$	0.9901	0.9900	0.9152	0.9150	0.9445	0.9445	0.9356	0.9356
$\lambda = 128$	0.9900	0.9899	0.9171	0.9168	0.9461	0.9463	0.9376	0.9376
CSEA L.S. + GNB								
$\lambda = 2$	0.9161	0.9167	0.8244	0.8264	0.9200	0.9196	0.9456	0.9456
$\lambda = \#classes$	0.9742	0.9742	0.8743	0.8724	0.9396	0.9396	0.9456	0.9456
$\lambda = 16$	0.9756	0.9755	0.8730	0.8703	0.9314	0.9321	0.9336	0.9336
$\lambda = 32$	0.9791	0.9790	0.8881	0.8867	0.9249	0.9259	0.9295	0.9295
$\lambda = 64$	0.9811	0.9811	0.8930	0.8920	0.9282	0.9290	0.9376	0.9376
$\lambda = 128$	0.9827	0.9826	0.8965	0.8950	0.9184	0.9194	0.9416	0.9416

1.2 Latent Space Visualization

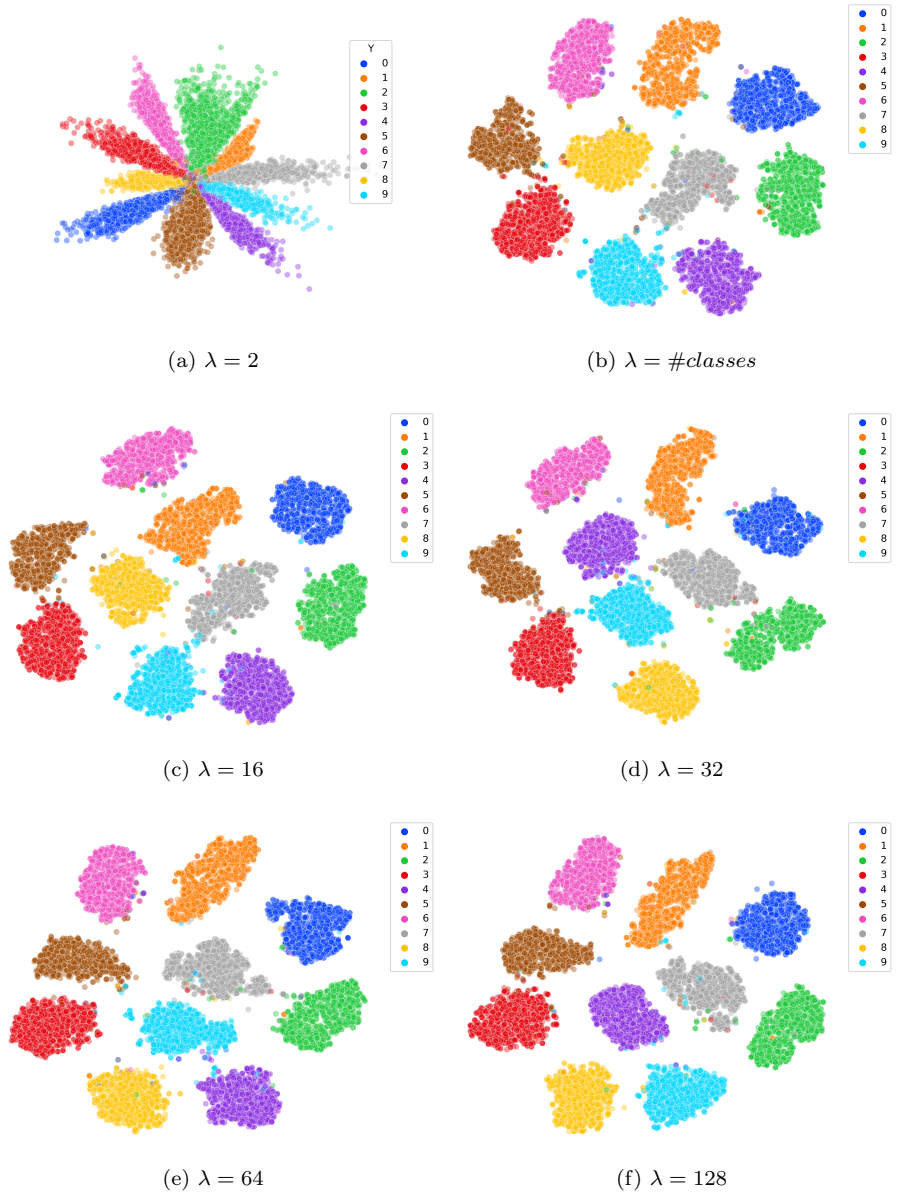


Figure 1: Scatter plot of the Latent Space created by CSAE for different number of dimensions (denoted as λ) for the MNIST dataset. For $\lambda > 2$, the Scatter Plot was constructed using the t-SNE algorithm.

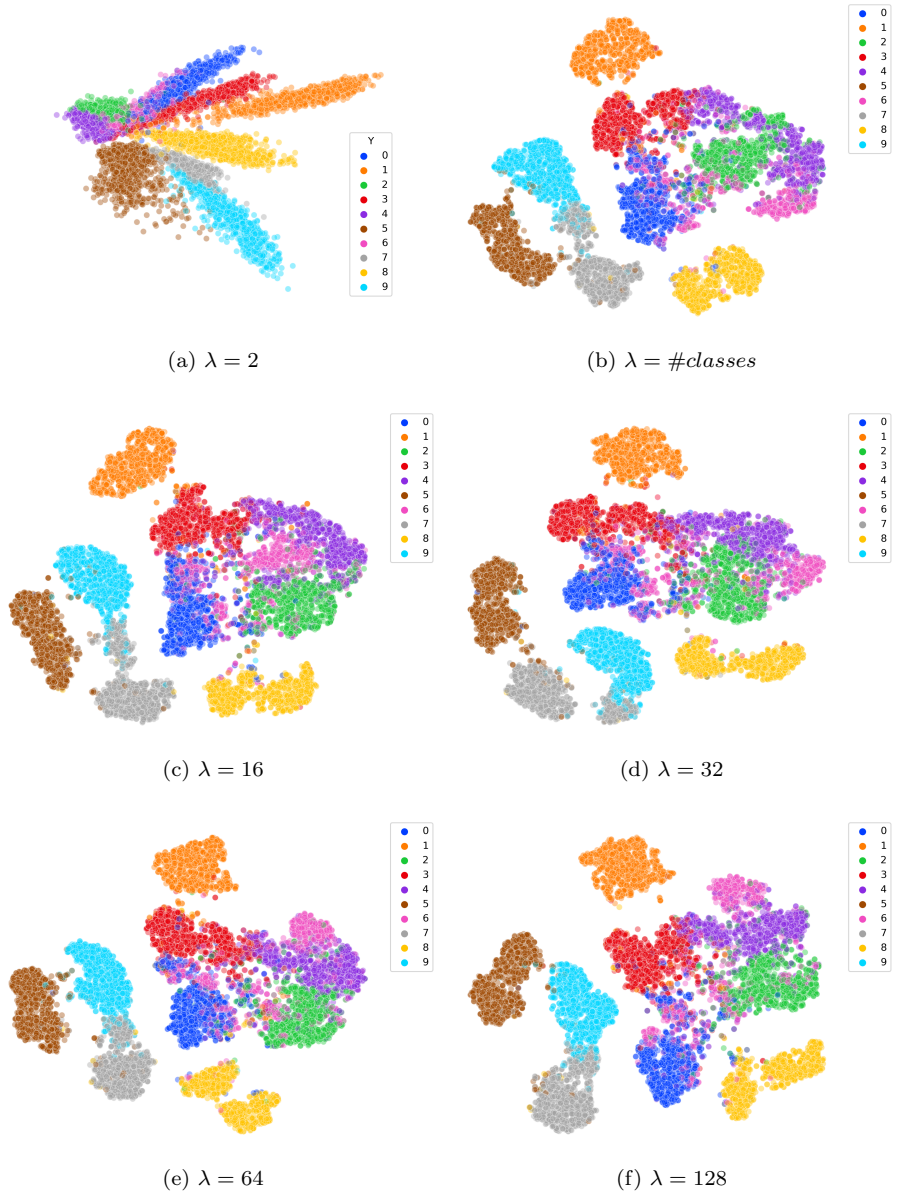


Figure 2: Scatter plot of the Latent Space created by CSAE for different number of dimensions (denoted as λ) for the Fashion MNIST dataset. For $\lambda > 2$, the Scatter Plot was constructed using the t-SNE algorithm.

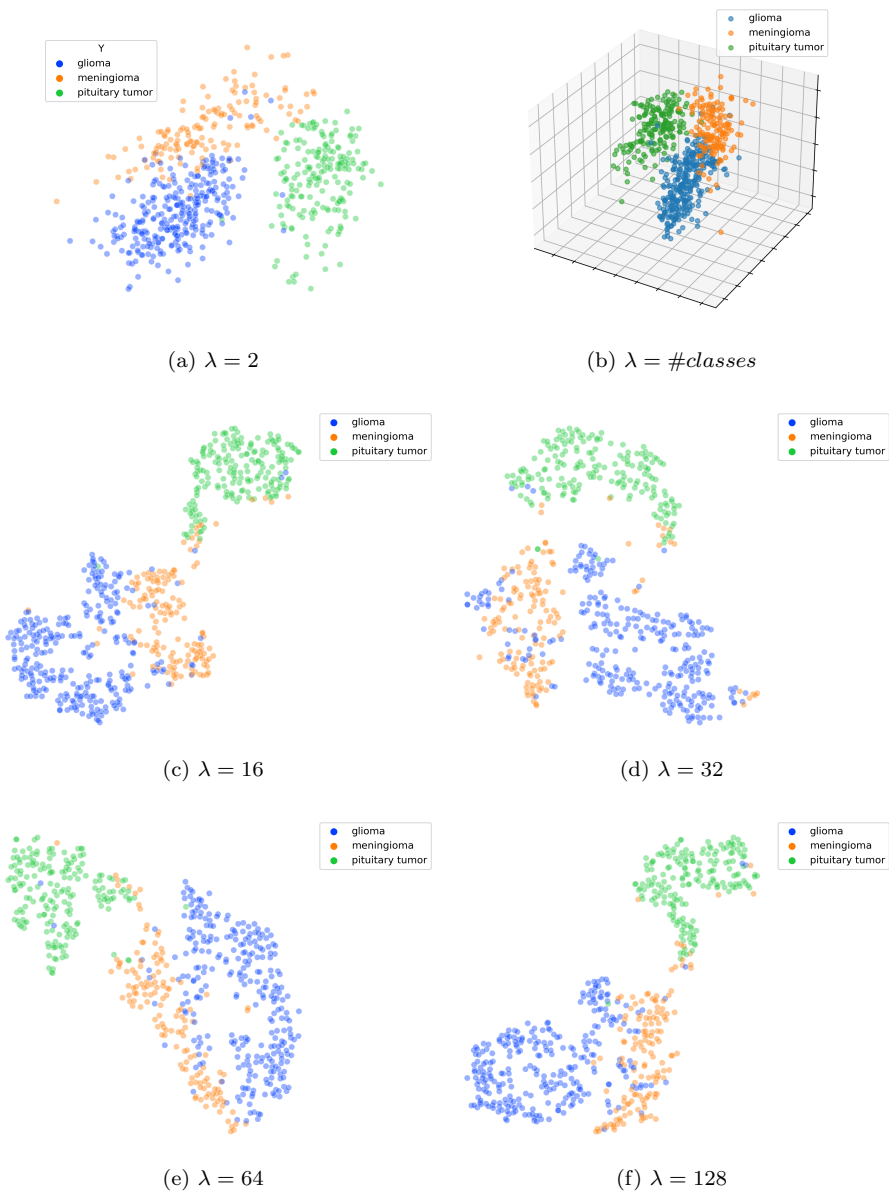


Figure 3: Scatter plot of the Latent Space created by CSAE for different number of dimensions (denoted as λ) for the Brain Tumor dataset. For $\lambda > 2$, the Scatter Plot was constructed using the t-SNE algorithm.



Figure 4: Scatter plot of the Latent Space created by CSAE for different number of dimensions (denoted as λ) for the SARS-COV-2 CT-Scans dataset. For $\lambda > 2$, the Scatter Plot was constructed using the t-SNE algorithm.